Environmental Science Nano

ROYAL SOCIETY OF CHEMISTRY

PAPER

View Article Online
View Journal | View Issue

Cite this: *Environ. Sci.: Nano*, 2024, 11, 2550

Unravelling mechanisms of CaO nanoparticle-induced drought tolerance in *Brassica napus*: an analysis of metabolite and nutrient profiling†

Ahsan Ayyaz,‡[a] Iram Batool,‡[a] Kangni Zhang,[a] Fakhir Hannan,[a] Yongqi Sun,[a] Tongjun Qin,[a] Habib-ur-Rehman Athar,[b] Zafar Ullah Zafar,[b] Muhammad Ahsan Farooq*[a] and Weijun Zhou *[a]

Nanotechnology has been widely used in agriculture to improve plant growth and stress tolerance. The exogenous application of calcium nanoparticles (CaO NPs) can improve plant tolerance to drought stress. However, the underlying physiological molecular mechanisms are still unclear. Herein, 100 mg L^{-1} of CaO NPs were applied to rapeseed plants when grown under the conditions of 0–15% w/v PEG-6000 solution. Drought stress reduced the rapeseed growth, CO_2 assimilation rate, stomatal conductance, and photosynthetic pigments. The application of 100 mg L^{-1} CaO NPs improved the growth of rapeseed plants under drought conditions (shoot dry weight, 77%; root dry weight, 69%). Growth improvement due to CaO NPs was positively associated with the photosynthetic rate, quantum yield of photosystem II and quantity of photosynthetic pigments. The net photosynthetic rate (Pn), stomatal conductance (Gs), internal CO_2 (Ci), and transpiration rate (Tr) increased by 65%, 85%, 69%, and 67%, respectively. The increases in quantum yield of photosystem II and photosynthetic pigments due to CaO NPs were 85% and 53%, respectively. A positive association between the growth and each of the gas exchange attributes, PSII activity and photosynthetic pigments indicated that CaO NPs improved the photosynthetic rate by reducing stomatal, as well as non-stomatal, limiting factors. The CaO NP treatment also improved the uptake of mineral nutrients under drought stress, including calcium by 82%, and potassium, phosphorous, magnesium, manganese, and boron by 78%, 89%, 72%, 80% and 73%, respectively. Furthermore, the application of CaO NPs caused a greater accumulation of 28 metabolites and reduced the accumulation of 18 metabolites that are mainly related to N-metabolism and amino acid biosynthesis, such as cysteine/homocysteine, lysine, tryptophan, alanine, glutamate, and proline, compared to droughted plants. The application of CaO NPs under drought conditions induced the up-regulation of upstream genes such as *CHS*, *CHI*, *F3′H*, and *F3H*, early development genes such as *PAL*, *C4H*, *4CL1*, *4CL5*, *DFR*, and *ANS*, and late development genes such as *UGT78D2*, *UGT79B1*, *MT*, *PAP1*, and *PAP2* in plants involved in flavonoid biosynthesis expression. The findings of this study suggest that CaO NPs improved the photosynthetic capacity through modulating the stomatal conductance, photosystem II activity, accumulation of nutrients, and reprogramming of both primary and secondary metabolic pathways such as N-metabolism, hormonal and flavonoid biosynthesis for regulating rapeseed growth under drought stress.

Received 29th January 2024,
Accepted 27th April 2024

DOI: 10.1039/d4en00080c

rsc.li/es-nano

Environmental significance

Nanotechnology has received significant attention for its diverse applications in industry, agriculture, and environmental remediation. The results of this study provide new insights into how CaO NPs regulate rapeseed growth under drought stress and allow us to better understand the CaO NP-mediated mechanism of *B. napus* by reprogramming the metabolome profile. CaO NPs resulted in the up-regulation of the expression of upstream genes involved in the biosynthesis of flavonoids, early and late development genes, and glycosyl-transferases, which are involved in the 3-*O*-glycosylation of flavonols and thus confirmed their role in plant growth and stress alleviation. This study provides compelling evidence for the use of nanomaterials in plant growth growing in water-affected areas.

[a] *Institute of Crop Science, Ministry of Agriculture and Rural Affairs Key Laboratory of Spectroscopy Sensing, Zhejiang University, Hangzhou 310058, China. E-mail: ahsanfarooq143@yahoo.com, wjzhou@zju.edu.cn; Tel: +86 571 88982770*

[b] *Institute of Botany, Bahauddin Zakariya University Multan, 40162, Pakistan*

† Electronic supplementary information (ESI) available. See DOI: https://doi.org/10.1039/d4en00080c

‡ These authors contributed equally.

1. Introduction

Agricultural production need to increase by 70% by 2050 to feed the world's 9 billion population. However, agricultural production, which is already low, is hampered by periodic drought stress and climate changes.[1,2] Therefore, the development of drought-tolerant crop cultivars or developing strategies to reduce the adverse effects of drought stress on crop production has become crucial. Drought affects plant development, crop growth, and yield.[3] Nano-particles have gained significant attention for their diverse applications in agriculture for crop improvement under stressful conditions.[4] However, engineered nanomaterials (ENMs) can benefit plant growth and development in unique ways depending on their physicochemical characteristics, applications, and concentrations.[5]

Calcium is a key component of cell walls and membranes and plays a role in the maintenance of normal cell structure and function.[6] It acts as a second messenger molecule in a variety of cell-signaling processes to reprogram the metabolic pathways and developmental programs under abiotic stresses.[7] Calcium deficiency reduces the plant antioxidant potential and photosynthetic efficiency (reduces F_m, F_v/F_m) in poplar plants.[8] Similarly, the deficiency of calcium causes cell membrane damage, decreased chlorophyll and chlorophyll precursor production, and decreased plant development in peaches.[9]

Previous studies have demonstrated that metal oxide nanoparticles (NPs) may reduce biotic and abiotic stressors, including water stress, in crops.[10] The application of potassium/silica and SiO_2 NPs to maize during drought conditions increases yield and growth.[11] Si and SiO_2 NPs also help barley that is suffering from drought.[12] Recently, a lot of attention has been paid to calcium-based nanomaterials because of their potential use for agricultural crops.[13] Recently, it was reported that CaO nanoparticles had a positive impact on barley growth under cadmium stress.[14] Similarly, in another study, 100 mg L^{-1} Ca-NPs resulted in higher bioaccumulation proportions of Mg, Mn, Ca, and N in rapeseed subjected to drought stress.[15] However, it is not well known how CaO NPs modulate nutrient uptake, either by increasing the selective uptake of nutrients through membrane transporters or by increasing the bioavailability of these nutrients in the rhizosphere. Similarly, there is a huge research gap in plants regarding how CaO NPs modulate primary and secondary metabolic pathways as they are the main growth determining factors. Metabolomics, or the global profiling of metabolites, is a potent tool for understanding the underlying mechanism of crop growth under normal or abiotic stress conditions.[16,17] Additionally, it is helpful for assessing any adverse effects of exogenously applied materials, including NPs, since such exposures might result in modest phenotypic changes that do not correspond to actual environmental risk.

Rapeseed is the fourth most extensively planted oilseed crop in the world, and the fifth biggest crop in China, with an annual planting area of 7.52 billion hectares.[18] *Brassica* species (*B. napus* L.) are economically and nutritionally significant across the world.[19] Its adaptability to different soil types, wide root system, rapid growth rate, increased biomass production, and greater resistance to environmental challenges make it a good candidate for drought-affected areas.[20] The current study investigated the potential of calcium oxide nanoparticles (CaO NPs) at 100 mg L^{-1} to mitigate the adverse effects of drought stress in rapeseed and elucidate the underlying mechanisms in plants. The current study has demonstrated that CaO NPs enhance drought tolerance in rapeseed by regulating the plant mineral nutrient status and photosynthesis capacity as evidenced by physiological studies complemented with metabolic profiles and gene expressions.

2. Materials and methods

2.1 Characterization of CaO NPs

The CaO nanoparticles were purchased from Shanghai Aladdin Biochemical Technology Co., Ltd. (CAT# 1305-78-8). The nano-calcium oxide particles were composed of CaO aggregates with organic material, so FTIR spectroscopy was used to detect the presence of functional groups on the surface of CaO NPs (model: Nico LET iS50 FTIR instrument). These functional groups can influence the interaction between nanoparticles and plant tissues. Understanding these interactions can help optimize the design of nanoparticles for specific agricultural applications. The morphological analysis and size distribution of CaO NPs was performed by using scanning electron microscopy (SEM) ZEISS Gemini SEM 300, Germany coupled with energy dispersion X-ray (EDX) spectroscopy to confirm the chemical composition of CaO NPs in their aggregates with organic material. The hydrodynamic size and zeta potential of CaO-NPs were measured using a NanoPlus "Particle Size & Zeta Potential Analyzer" (Particulate Systems is a subsidiary of Micromeritics, 4356 Communications Drive, Norcross GA, 30093, USA) at a scattering angle of 90° at 25 °C.[13]

2.2 Experimental plan and growth conditions

The seeds of rapeseed (*B. napus*) cultivar ZD622 were uniform and of high quality, obtained from the College of Agriculture and Biotechnology, Zhejiang University, China. The seeds were cultured in a half-strength Hoagland nutrient solution. After germination, the uniform-sized seedlings were transferred to half-strength Hoagland nutrient solution in plastic pots. After two weeks, the seedlings were used for 100 mg L^{-1} CaO NP treatments for one week before drought (15% PEG-6000 w/v) treatment in full-strength Hoagland. Leaf samples were taken after seven days of drought treatment. The samples were immediately frozen in liquid nitrogen and kept at −80 °C. Each treatment consisted of three biological replicates.

2.3 Confocal microscope imaging

Plant leaf samples were sectioned with a microtome and kept for about 30 min in 1% rhodamine, then passed 3 times through distilled water. The perforated pieces were put on glass slides and viewed with a water immersion objective lens (Olympus LUM Plan FLN) with a mode-locked Ti : sapphire laser (Spectra-Physics, Mai-Tai HP). Samples were excited with the 488 nm line of an argon laser, and dye emission was collected at 400 to 520 nm. Rhodamine alone was used to check the background fluorescence due to the non-specific binding of rhodamine. The DCF fluorescence was visualized in a single optical section of the leaves. All images were obtained at the same depth.[21,22]

2.4 Photosynthetic pigment measurements and gas exchange parameter measurements

Photosynthetic pigments were estimated by following the standard method,[23] using a spectrophotometer (Hitachi F-4600, Japan). Similarly, the analysis of gas exchange parameters was performed by using a portable photosynthesis apparatus LI-COR 6400XT.[24] The detailed procedures for measuring photosynthetic pigments and gas exchange parameters are provided in the ESI† S1.

2.5 Macro- and micro-nutrients, and the structural stability of PSII using O-J-I-P analysis

Leaves of *B. napus* were ground into powder and mixed with 31% HNO_3 with 17.5% H_2O_2 for digestion on a hot plate at a moderate temperature, *i.e.*, 250 °C for 2 hours, after which the samples were cooled to room temperature. In digested leaf samples, macro- and micronutrients were measured using an inductively coupled plasma mass spectrometer (ICP-MS).[25]

The FlourPen (FP 100, Photon System Instruments, Czech Republic) is a commercially available device used for measuring the OJIP curves. Leaves were dark-adapted for 20 minutes using leaf clips prior to OJIP measurements. Raw data were processed to estimate the JIP-test parameters using the FluorPen software version 2. JIP test parameters were measured using formulae as described elsewhere.[26,27] The detailed JIP test formulae are provided in the ESI† S1.

2.6 Metabolomics data analysis and the processing of rapeseed plants

For the evaluation of metabolomics analysis, six biological replicates of about 20 mg each of the rapeseed frozen leaf tissues were ground using a tissue lyser in 1 : 1 methanol and water. The milled leaf tissue material was precipitated, stored at −20 °C for about 3 hours, and centrifuged for 25 min at 30 000 × *g*, 4 °C. After centrifugation, about 550 μL of supernatant was gently transferred to new tubes. The samples were analyzed and identified for their components using liquid chromatography-mass spectrometry (LC-MS). Initially, chromatographic separations were obtained and observed using high-performance liquid chromatography (2777C UPLC system, Waters, UK). In detail, a 20 μL aliquot of each sample was separated using an ACQUITY UPLC@HSS T3 column (100 mm diameter, 1.8 mm film thickness, Waters, UK), at a constant temperature of 50 °C. The separation system was comprised of a mobile phase in the form of solvent A having 0.2% formic acid + water, and solvent B with 0.2% formic acid + acetonitrile. For the elution gradient, the conditions were kept constant for 0–5 min, 100% phase A, 2–15 min, 0–100% phase B, 15–17 min, 100% phase B, 17–20 min, 0–100% of phase A, with a flow rate of 0.5 ml min^{-1}. Then, the eluted samples were subjected to metabolites analysis using a high-performance tandem mass spectrometer (Xevo G2 XS QTOF, Waters, UK), operating both the positive and negative ionic modes at a sampling cone voltage of 40 V, while the capillary voltage was kept constant at 3 kV and 2 kV for the positive and negative modes, respectively. Spectroscopy data were obtained in the centroid MSE mode by keeping the time of flight at 50–1200 Da and scanning time of 0.3 s. All of the precursors were fragmented at 20–50 eV and detected (MS/MS) in a time span of 0.4 s. For the calibration of the LC-MS system, the LE signals and quality control samples were observed every 3 s.

2.7 Quantitative real-time PCR analysis

For the extraction of total RNA from fully frozen leaf samples of all treatments, the TRIzol (Tiangen Biotech, Beijing, China) method was used, and RNA reverse transcription was performed by using the FastKing RT Kit (Tiangen Biotech).[28] The detailed procedure for the real-time PCR analysis is provided in Table 1.

2.8 Statistical analysis

In this study, all the data are presented in terms of means ± S.E. To compare treatments, two-way ANOVA was performed the means were compared using an LSD test at a 5% significance level, by using the GraphPad Prism 7.0 software.

3. Results and discussion

3.1 Calcium nanomaterial characterization and translocation *B. napus*

CaO NP characterization is presented in Fig. S1A–F,† which includes morphological and physicochemical examination from SEM-EDS, zeta potential, FTIR, and XRD. CaO NPs exhibited a spherical morphology with an average particle size of 85 nm, a hydrodynamic size of 244 nm, and a zeta potential of +28 mV, (Fig. S1A–C†). In line with previous studies, the FTIR spectra covered a wide range of 400 to 4000 cm^{-1}.[14] In the FTIR spectrum, the larger peaks at 3643, 3448, 1794, 1637, 1429, and 1114 cm^{-1} represent the stretching of the alcohol O–H group, C═C, C═O stretching, the existence of the CH_2 polysaccharide functional group, and (P–O–C) bonding (Fig. S1D†). FTIR is a very versatile tool for surface characterization of nanoparticles. Under specific conditions,

Table 1 List of primers used for qRT-PCR analysis

Primer name	Primer sequence from 5′ to 3′
BnActin′F	GATTCCGTTGCCCTGAAGTA
BnActin′R	GCGACCACCTTGATCTTCAT
PAL F	GAAGATTACAGAAAAGGTGCGG
PAL R	CGGCGTTCAAGAACCTAATAAG
C4H F	GACTTTAGGTATGTGCCGTTTG
C4H R	AATCGTGATTCCCAAAATAGGC
4CL1 F	ATACAGAGGTGTAAAGTGACGG
4CL2 R	GATTTCACAACCCTAATCGAGC
4CL2 F	GGAGACGGAGAAGTATGATCTG
4CL2 R	GAAACTTAGCACTGATGGCATC
4CL3 F	TTGGGTATGTTGACGAAGATGA
4CL3 R	GTTTCCATTTGATCGGACTACG
4CL5 F	AGTGTCCGGAAAGATTCTTAGG
4CL5 R	GCGTTGGAGCTTACACATTTAT
CHS F	CTTGCATACTACACAAGATCGC
CHS R	GCGGAAGTAGTAGTCTGGATAC
CHI F	AGAAAGTAACGGAGAACTGTGT
CHI R	TGAAGACTTCCAAGAACCTCTC
F3′H F	GAAAGGAAACGATTTCGAGCTT
F3′H R	CCGAGTCCATAAGCACTCATAT
F3H F	AAAAGAGGAGAGATCTGTCGTC
F3H R	TATCGGCCACCAAACTAGTATC
DFR F	GCTCTCTCCTATCACTCGTAAC
DFR R	ATTGCATAAATCGTCCAAGTGG
ANS F	CACGAGTGAGTACGCTAAGTAT
ANS R	CCAACTTCTTTCTCTAGACGGT
UGT78D2 F	CTCTGTTTTCTCAGACACGTTG
UGT78D2 R	ATAACGCGAGAGGACCAATATT
UGT79B1 F	GGTGCTAAAACTGTTTGCTACA
UGT79B1 R	CATTTCCTTCCCGTCAATGATC
MT F	GCCTACGTCATAACATGTTTGG
MT R	GACAATGCAGTTCCCGAAATAC
PAP1 F	GCCAAAAGTTGACGTTATTCCT
PAP1 R	GTTGCTAGCTTTTCTGTCTCTG
PAP2 F	AAAGGTACGGCAACAAAAATGG
PAP2 R	AGTTCTACAGTCTCTCCATCCA
PAP3 F	GCGACGATAAAAGTTGAGTGTT
PAP3 R	GAAGAAGGAGACAAAATCGACG

the NP surface chemical composition can be determined, and the reactive surface sites responsible for the surface reactivity can be identified. FTIR spectroscopy is used to identify the characteristic functional groups from the spectral bands, which allowed us to determine the conjugation between the nanomaterial and the adsorbed biomolecules.[29,30] These findings showed that the role of functional groups is essential for the nanoparticles' capacity to modify their structural and functional properties, which in turn affects how they react and behave on the surface, how hydrophilic they are, and how active they are electrically or catalytically. FTIR spectra consist of absorption peaks that correspond to the frequencies of vibrations between the bonds of atoms in the nanoparticles.[29] The crystalline planes and crystalline character of the Ca-NPs were demonstrated by the XRD spectra (Fig. S1E†). XRD is used for the characterization of nano-powders of any size, and the observed changes in positions of diffraction peaks are used to make conclusions on how the crystal structure and cell parameters change with the changes in nanoparticle size and shape. The diffraction peaks of Ca-NPs were observed at 18.84°, 29.66°, 34.80°, 47.17°, 51.86°, 54.68°, and various diffraction angles of Ca-NPs at 2θ degrees coincided at 110, 200, 211, 314, 222, and 319, respectively. The cubic phase of Ca-NPs with a space group of $Fm\bar{3}$ is consistent with the standard JCPDS File No. 37-1497.[14,29,31] These results are in line with previous studies.[30–32] The EDS analysis further confirmed the elemental composition of CaO NPs as revealed by X-ray spectroscopy SEM-EDS as shown in Fig. S1F and S2.† EDS can effectively measure trace concentrations of CaO in materials. With proper calibration, sample preparation, and careful analysis techniques, EDS can provide accurate and reliable results for even trace elemental analysis in nanoparticle samples.

To visualize the uptake and distribution of Ca-NPs in leaf tissues, we treated plants with 1% rhodamine fluorescent dye and observed their distribution *via* confocal laser scanning microscopy (Fig. 1A–I). Confocal microscopy is primarily used for imaging at the cellular and subcellular level; it can be adapted to identify nano-sized structures with appropriate modifications and techniques.[22,32] These techniques include resolution enhancement techniques, multiphoton excitation, fluorescence labeling, nanoscale imaging probes, super-resolution techniques and functional imaging. The results obtained are consistent with the confocal microscopy of CaO NP results from previous studies.[22,31–33] In the current study, the fluorescent dye allowed us to clearly trace the entry of Ca-NPs and their distribution within the leaf tissue. According to the data, Ca-NPs accumulated inside the rapeseed leaf tissues. The accumulation of Ca-NPs was evaluated in all parts of the cells in control plants without drought stress. According to the data, we found fluorescence signals of the CaO NPs in the intercellular spaces of leaves, chloroplasts, guard cells, and stomata (Fig. 1D–I). This widespread distribution within the leaf suggests potential interactions with different cellular structures and processes. In line with previous studies, the current study found that the nanoparticle charge and size controlled the foliar delivery efficiency to plant cells and organelles.[34] NPs can enter leaf tissue *via* the cuticle or stomata. Water-suspended nanoparticles can enter plant cuticles through aqueous pores with effective sizes of 0.6–0.8 nm. The confocal laser images showed that Ca-NPs were absorbed by rapeseed leaves and distributed in the inter-cellular spaces of the leaves, chloroplasts, and guard cells. Moreover, the leaf tissue images revealed the normal stomatal length density and Ca-NP distribution (Fig. 1I). In addition, the leaf ultrastructure showed and confirmed the uptake and accumulation of CaO NPs in leaf tissue (Fig. 1J). Furthermore, SEM-EDS analysis revealed the purity of CaO NPs with high levels of Ca and O in the material used in this study (Fig. 1K and L). EDS can effectively measure trace concentrations of CaO in materials. With proper calibration, sample preparation, and careful analysis techniques, EDS can provide accurate and reliable results for even trace elemental analysis in CaO-containing samples.[34,35] The results obtained are consistent with the confocal microscopy of CaO NP results in previous studies.[31]

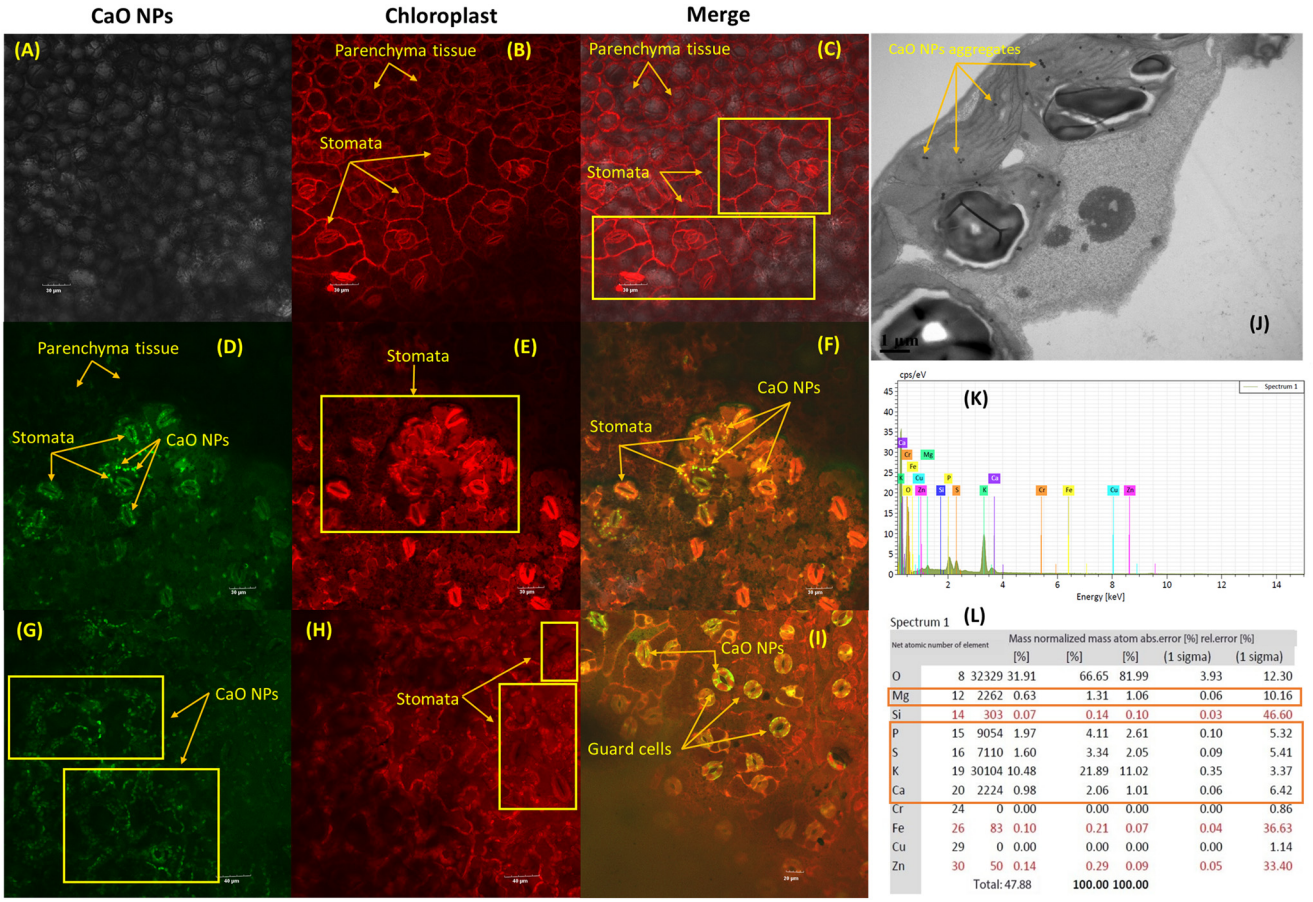

Net atomic number of element			Mass normalized mass atom abs.error [%] rel.error [%]				
			[%]	[%]	[%]	(1 sigma)	(1 sigma)
O	8	32329	31.91	66.65	81.99	3.93	12.30
Mg	12	2262	0.63	1.31	1.06	0.06	10.16
Si	14	303	0.07	0.14	0.10	0.03	46.60
P	15	9054	1.97	4.11	2.61	0.10	5.32
S	16	7110	1.60	3.34	2.05	0.09	5.41
K	19	30104	10.48	21.89	11.02	0.35	3.37
Ca	20	2224	0.98	2.06	1.01	0.06	6.42
Cr	24	0	0.00	0.00	0.00	0.00	0.86
Fe	26	83	0.10	0.21	0.07	0.04	36.63
Cu	29	0	0.00	0.00	0.00	0.00	1.14
Zn	30	50	0.14	0.29	0.09	0.05	33.40
		Total: 47.88		100.00	100.00		

Fig. 1 Illustration of the leaf cellular distribution of CaO NPs under control and drought stress treatment, observed *via* a laser confocal microscope. Arrows represent chloroplasts, stomata, and guard cells. Scale bars represent 30–40 μm. (A–C) CK (10× objective), (D–F) 100 mg L^{-1} CaO NPs with a 10× objective, (G–I) 100 mg L^{-1} CaO NPs under drought stress (10× objective). (J) The uptake and transport confirmation of CaO NPs in the form of aggregate formation in *B. napus* leaves. (K and L) The mineral element composition of CaO NPs observed through SEM-EDS and their percentages, respectively.

It was reported that the foliar spraying of 50, 100 and 150 μM Si-NPs significantly increased Si concentration in *B. napus* leaves and roots.[31] These findings support the hypothesis that foliar application of CaO NPs can penetrate leaf tissue *via* the stomatal opening, accumulate in rapeseed plants, and take part in plant growth and development.

3.2 CaO NPs improve plant growth and PSII activity under drought stress

The foliar application of CaO NPs to rapeseed seedlings under drought showed a positive effect on plant growth in terms of increased biomass accumulation, photosynthesis indices and mineral acquisition (Fig. 2 and 3). The 100 mg L^{-1} CaO NPs treatment under drought conditions significantly improved the shoot fresh weight by 70%, root fresh weight by 66%, shoot dry weight by 77% and root dry weight by 69%, as compared to drought-treated plants (Fig. 2A–D). Drought treatment exhibited a marked decrease in the plant shoot fresh weight by 63%, root fresh weight by 57%, shoot dry weight by 74% and root dry weight by 82%, with respect to the control plants (Fig. 2A–D). Recent studies demonstrated that the application of metallic nanoparticles could improve plant growth and stress tolerance.[36,37] Further mechanistic studies revealed that increased plant growth occurred through $^{\cdot}OH$ radical-mediated cell wall loosening *via* CaO NP action. Consistent with our findings, calcium phosphate nanoparticles increased the rice seedling growth and stress tolerance.[38] In the present investigation, CaO NPs increased root growth by lowering the PEG-6000-induced phytotoxic impact on plants, resulting in the loss of adverse effects on root elongation. However, a supplement of 100 mg L^{-1} CaO NPs to plants significantly improved plant growth as observed through metabolomics.

According to the findings, CaO NP treatments exhibited a considerable increase in the amplitude of OJIP curves as compared to control plants following drought stress. Likewise, CaO NPs regulated the PSII performance of drought-stressed rapeseed plants by regulating the energy of absorption, trapping and electron transport beyond Q_B in terms of quantum efficiencies or energy fluxes per reaction center, such as ψ_o, Φ_{Eo}, Φ_{Do}, ABS/RC, TRo/RC, ETo/RC, and

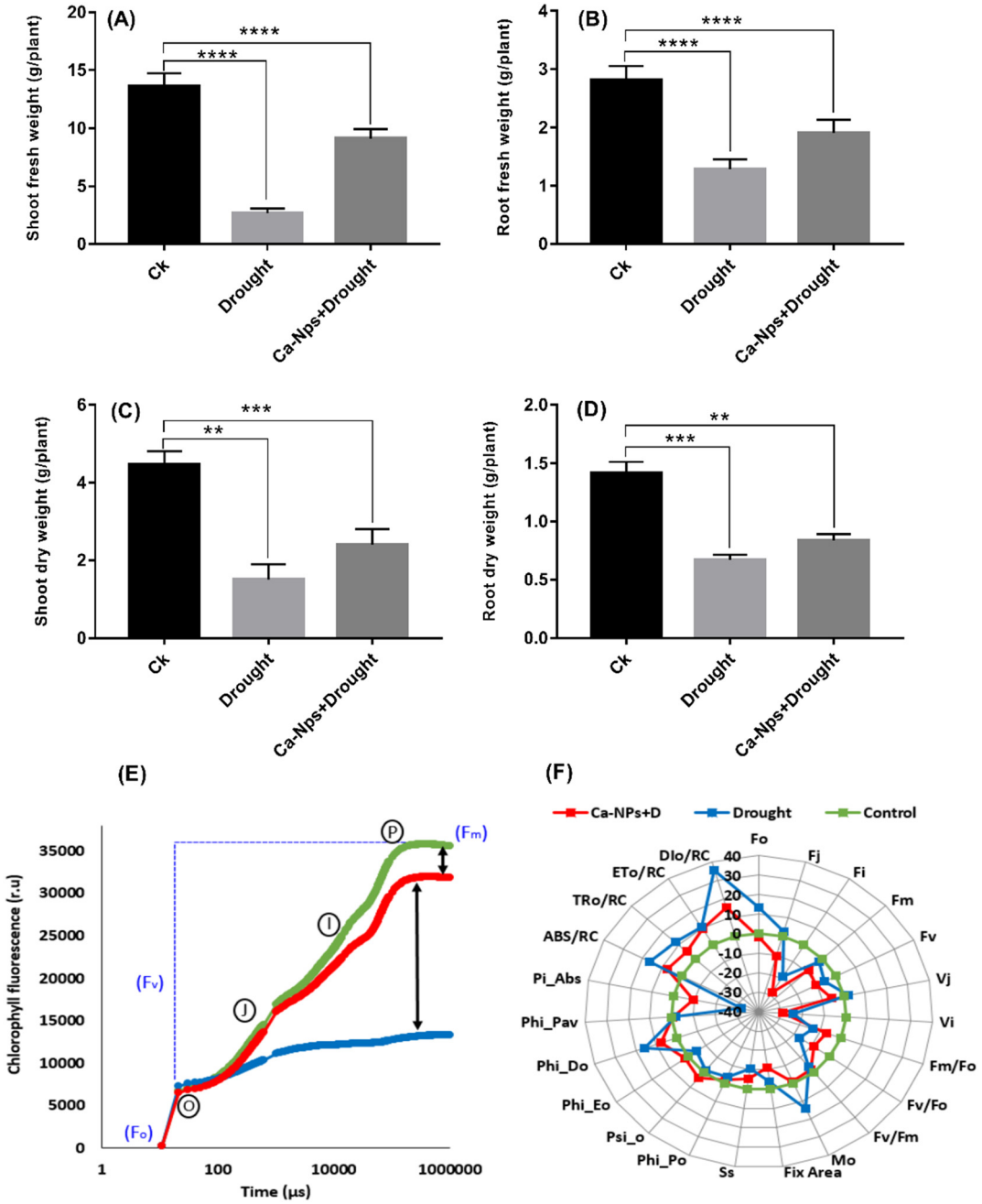

Fig. 2 The effects of CaO NPs (100 mg L^{-1}) on rapeseed growth and PSI performance following drought stress (15% PEG-6000) for seven days. (A and B) Shoot and root fresh weight, (C and D) shoot and root dry weight, (E) chlorophyll fluorescence relative values, and (F) a radar plot showing PSI-related parameters through the OJIP chlorophyll fluorescence test. Means were compared using an LSD test at a 5% significance level; the significance levels are represented as follows: * = 0.05, ** = 0.01, *** = 0.001, **** = 0.0001, ns = non-significance.

DIo/RC (Fig. 2E and F). The regulation of energy absorption is key to maintaining PSII structural stability and functional activity, the overall light reaction and photosynthetic capacity, and cellular redox balance, which translate into plant growth and productivity under stressful conditions.[39] The optimal method for evaluating PSII efficacy involves measurements of PSII activity through OJIP analysis or induction curve analysis of plants grown under controlled and stressed conditions[40] and typically exhibits a strong correlation with plant biomass.[41] In contrast, CaO NPs-treated plants grown under drought stress exhibited a substantial increase in Φ_{Pav} (Fig. 2F), which is analogous to previous studies in which it was demonstrated that a 50 mg L^{-1} GO application increased the quantum yield of PSII (F_v/F_m) and the actual efficiency of PSII in droughted *Aloe vera* plants.[42] Similarly, the addition of CaO NPs increased the maximum number of turns over (N) and the rate of Q_A reduction (M_o) until the maximum fluorescence (F_m) was

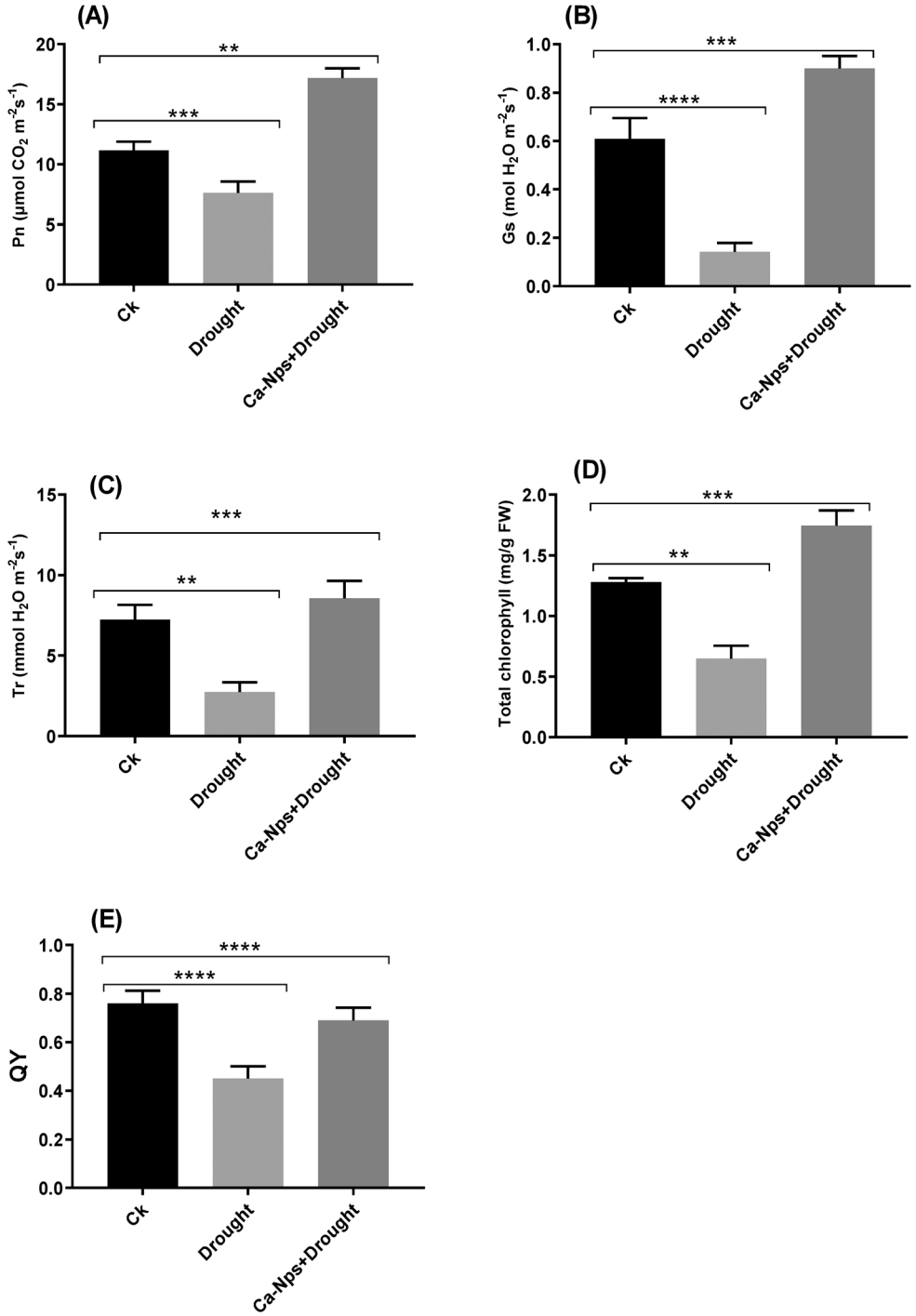

Fig. 3 The responses of rapeseed to CaO NPs (100 mg L^{-1}) and drought on gas exchange indices, QY of PSII and mineral nutrient profile of rapeseed following drought stress (15% PEG-6000) for 7 days. (A) The net photosynthesis rate (Pn), (B) stomatal conductance (Gs), (C) transpiration rate (Tr), (D) total chlorophyll content, (E) QY of PSII. Means were compared using an LSD test at a 5% significance level; the significance levels are represented as follows: * = 0.05, ** = 0.01, *** = 0.001, **** = 0.0001, ns = non-significance.

reached, which indicated that CaO NPs enhanced the electron transport flux from PSII to further than Q_A, similar to earlier studies.[15] CaO NPs also facilitated the considerable increment of dissipation energy flux per reaction center (DIo/RC), although a decrease in energy flux per reaction center was more obvious in drought-treated plants.[25] According to our results, CaO NPs had a positive impact on the structural stability of PSII as evidenced by a reduction in F_o, L and K bands (a measure of the energetic connectivity of the antenna and oxygen-evolving center with the reaction center). Our results in Fig. 2F show that CaO NPs contributed to the changes in the parameters of quantum performance and total chlorophyll content. Ca-NPs helped in the regulation of the transfer of electrons from PSII to the final acceptors of PSI as

observed earlier.[43] The physiochemical properties of CaO NPs such as high electronic conductivity, high surface area and mechanical strength enabled the nanoparticles to act as effective delivery systems for plant cells and tissues that improved plant growth and stress tolerance.[15]

3.3 CaO NPs regulate gas exchange indices, chlorophyll content and nutrient uptake

Drought stress suppressed the gas exchange attributes (Pn, Gs, Ci, Tr), total chlorophyll and QY of PSII of rapeseed plants by 76%, 89%, 72%, 82%, 89%, and 38%, respectively (Fig. 3A–E). The application of 100 mg L^{-1} of CaO NPs resulted in an increase in photosynthetic rate, stomatal conductance, sub-stomatal CO_2, total chlorophyll, and QY of PSII by 65%, 85%, 69%, 85% and 53%, respectively (Fig. 3A–E). Drought stress reduced water transport from root to shoot caused by stomatal closure, hindered the influx of CO_2 and thus the photosynthetic rate, which is parallel to the findings of some previous studies.[44,45] The exogenous application of Ca-NPs improved the photosynthetic pigments and photosynthetic rates by improving stomatal conductance, which is similar to several studies in which the exogenous application of growth regulators or antioxidants improved photosynthetic rates by reducing stomatal limitations[39,46] (Fig. 3A–E). In drought-stressed rapeseed plants, ZnO NPs enhanced the PSII activity, which is in line with some earlier studies with wheat where it was demonstrated that exogenous application improved PSII activity and the photosynthetic rate.[47] Plants treated with calcium nanoparticles demonstrated increased cell membrane structural integrity and preserved membrane function for ion homeostasis.

Drought stress reduced nutrient uptake in rapeseed plants as follows: calcium was reduced by 74%, potassium by 67%, phosphorous by 61%, magnesium by 85%, manganese by 76% and boron by 81%, (Table 2). CaO NP treatment increased the uptake of mineral nutrients as follows: calcium by 82%, potassium by 78%, phosphorous by 89%, magnesium by 72%, manganese by 80% and boron by 73% under drought stress (Table 2). Enhanced nutrient uptake and efficient use capacity might help in mitigating the devastating impacts of drought. Nutrient shortage has different consequences on plant metabolism and growth. Drought reduces the nutrient uptake and transport from root to shoot, even when the soil is not deficient in nutrients.[37] Consistent with previous studies on sorghum and cucumber, the use of zinc oxide nanoparticles enhanced the nutrient uptake and accumulation in the leaves and roots of drought-stressed plants.[36,37]

3.4 Metabolomics profile analysis

The 324 deferentially expressed metabolites were identified in rapeseed plants following the CaO NPs and drought treatment as shown in Table S1.† A multivariate method using principal component analysis (PCA) revealed that samples from the same group were classified in combination, in either positive (ESI + ve) or negative (ESI − ve) ion detection mode (Fig. 4A–D). All of the plant samples were split into control, drought, and CaO NP treatments, indicating a noticeable metabolomics change in response to drought stress. Plants growing under control conditions showed differential effects on the rapeseed metabolism profile, implying that the drought and CaO NPs treatments had innate variations in metabolomics composition. Plants subjected to CaO NPs exhibited a significant change in metabolite expression compared to the control plants (Fig. 4E and F; Table S2†). As a result, the CaO NP treatment affected the metabolomics signature in drought-stressed rapeseed seedlings. Furthermore, PLS-DA data demonstrated that the CaO NP had a greater effect on metabolite expression under drought as compared to control plants, as validated by PC scores under either ESI + ve (Fig. 4E) or ESI − ve (Fig. 4F) mode. Even though plants subjected to CaO NPs displayed significant differences in metabolite expression compared to control plants, the clarity was enhanced by using a supervised multivariate technique based on partial least-squares discriminant analysis (PLS-DA); as a result, it is obvious that CaO NP treatment affected the metabolomics signature in drought-stressed rapeseed seedlings. Furthermore, PLS-DA data demonstrated that CaO NP had a greater effect on metabolite expression under drought conditions as compared to control plants, as validated by PC scores under either ESI + ve or ESI − ve (Fig. 4E and F) mode.

Several metabolites, including phenols and derivatives (5), amino acids and derivatives (31), terpenoids (16), organic acids (11), lipids (24), nucleotide (5), and carbohydrates (6), and benzene and derivatives, alkaloids, coumarins and steroids related metabolites (11, 6, 8, and 5), showed differential expression in rapeseed seedlings (Fig. 4G and H; Table S3†). According to the data, most of the CaO NP-responsive metabolites showed up-regulated expression related to amino acids and lipids, followed by carbohydrates and nucleotides in rapeseed seedlings following drought stress (Fig. 4G and H; Table S4†). The CaO NP treatment up-regulated the expression of 17 metabolites related to amino acids, peptides, and analogues, majorly including cysteine, tryptophan, glycine, alanine, phenylalanine, glutamate,

Table 2 The effects of CaO-NPs on the mineral profile of rapeseed under drought stress

Treatments	Ca (mg kg^{-1} DW)	Mg (mg kg^{-1} DW)	K (mg kg^{-1} DW)	Fe (mg kg^{-1} DW)	Cu (mg kg^{-1} DW)	Mn (mg kg^{-1} DW)	Zn (mg kg^{-1} DW)
Ck	8.589783	10.35334****	30.2	0.03	0.006837	0.045	0.019
Drought	5.6**	6.6****	20.35****	0.01	0.001***	0.02	0.01
Ca-Nps + drought	9.7****	14.23****	38.24****	0.045	0.0095***	0.055***	0.04

The significance levels are represented as * = 0.05, ** = 0.01, *** = 0.001, **** = 0.0001.

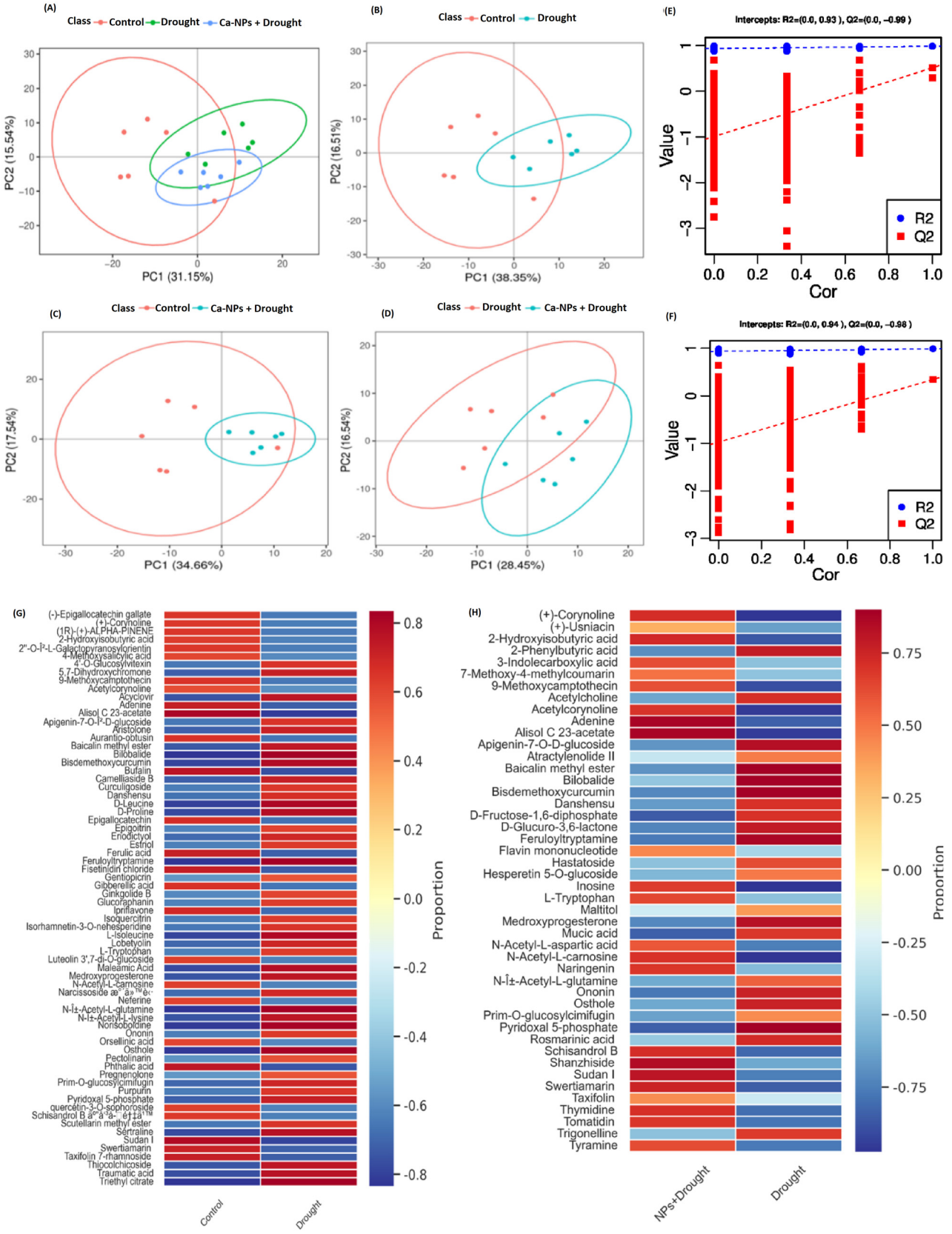

Fig. 4 The metabolite abundance in rapeseed leaves upon exposure to CaO NPs + drought stress conditions (foliar application of 100 mg L^{-1} CaO NPs and 15% PEG-6000). Principal component analysis (PCA) score scatter plot model for all observed metabolites in the (A–D) control and drought conditions; the scatter color indicates the different experimental groups. (E and F) Data are provided for both positive (ESI + ve) and negative (ESI − ve) ion detection modes. The PLS-DA model for all detected metabolite features in (G) control *vs.* drought, and (H) drought *vs.* CaO NPs + drought stress conditions following foliar treatment with 100 mg L^{-1} CaO NPs and 15% PEG-6000 for 7 days.

proline, and homocysteine, and down-regulated the expression of 4 metabolites including serine and leucine (Fig. 4H). According to the literature, glycine is a sign of changed photo-respiratory carbon and regulates both plant development and photosynthesis.[48,49] Iron–sulfur clusters are crucial parts of electron transport proteins, and cysteine is a significant source of sulfide.[50] Consistent with our findings, it was proposed that the degradation of metabolites related to amino acid metabolism affects several key amino acids, including aspartic acid, glutamic acid, leucine, L-tyrosine, and lysine. This could have significant implications for various physiological processes and metabolic pathways associated with these amino acids.[51] Interestingly, CaO NP-treated plants showed a good proportion of lipids with 22 up-regulated and 2 down-regulated metabolites mainly including maltitol, 2,2-dimethylesuccinic acid, 6-aminocaproic acid, traumatic acid, gibberellic acid, and tomatidine (Fig. 4H). Additionally, it was shown that the CaO NP treatment increased the expression of metabolites such as glycerol, L-arabitol, and D-fructose-1,6-diphosphate, which are involved in the metabolism of carbohydrates (Fig. 4H).

According to the findings, glycerol, which is a precursor of glycerol-3-phosphate (G3P), encourages plant growth and resilience.[52] These metabolites additionally participate in

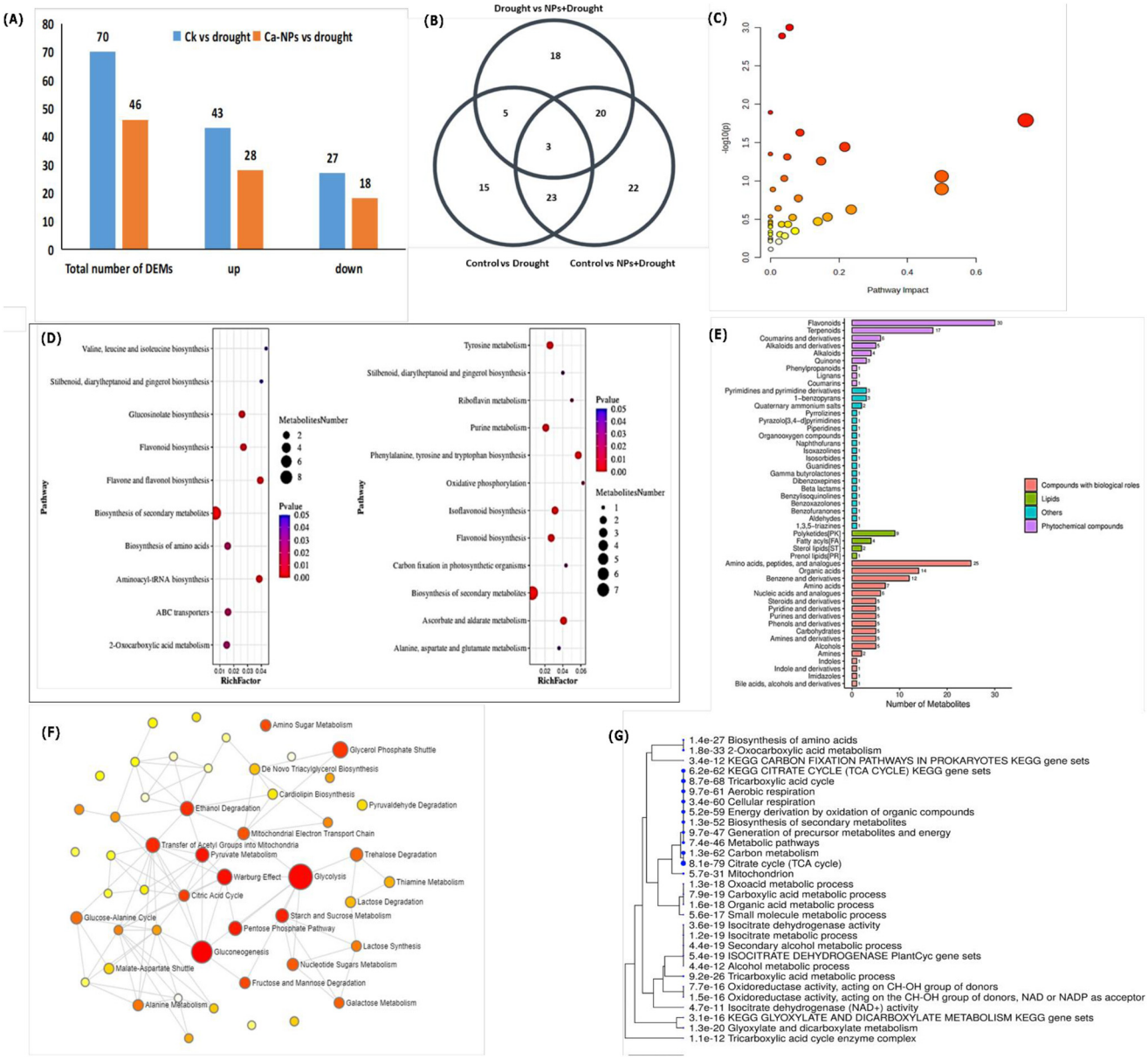

Fig. 5 The effects of foliar application of 100 mg L^{-1} CaO NPs on rapeseed under 15% PEG-6000 treatment for 7 days. (A) Differential metabolite expression. (B and C) Venn diagram of changed differential metabolites and pathway impact. (D and E) The general profile of rapeseed metabolite control in primary and secondary metabolism. (F and G) The network interaction analysis of GO terms that were upregulated DEGs (red nodes and edges) and downregulated DEGs (green nodes and edges) enriched in the GO biological process, cellular component and molecular functions and GO molecular functions associated with DEGs modulated in rapeseed primary and secondary metabolism.

energy-producing processes such as glycolysis and glycerolipid synthesis, making them plant defense-signaling regulators. In response to abiotic stress, fructose acts as a plant signaling molecule, influencing physiological functions such as photosynthesis, seed germination, and flowering.[53] Importantly, metabolomics research has demonstrated considerable down-regulation of low molecular weight antioxidants, plant growth promoters, and stress-resistant components due to CaO NP exposure at both levels, all of which may damage the antioxidant and defense system of the plant. The relevance of these detrimental metabolomics alterations could become clear over a longer period or possibly in the field with exposure to concurrent stressful conditions.

3.5 Differential expression of metabolites and KEGG pathway enrichment analysis

In comparison to control plants, 43 metabolites were up-regulated and 27 metabolites were down-regulated under drought stress (Fig. 5A). In contrast, CaO NP treatments showed the up-regulation of 28 metabolites and down-regulation of 18 metabolites as compared to drought-stressed plants (Fig. 5A). Furthermore, CaO NP treatment under drought conditions showed 22 differential metabolites as compared to control plants (Fig. 5B). These findings, however, point to the existence of a conserved metabolic signature in rapeseed seedlings that is impacted by Ca-NPs (Fig. 5C). CaO NPs work as indispensable elements for certain physiological and biochemical processes and play a pivotal role in improving plant growth and drought tolerance.[54]

The majority of the metabolites found in the studied rapeseed under drought conditions were due to the biosynthesis of secondary metabolites, flavonoid biosynthesis, and the biosynthesis of amino acids such as valine, leucine, and isoleucine as shown in Fig. 5D. The supplementation of CaO NPs showed a high expression of metabolites involved in the biosynthesis of secondary metabolites, alanine, aspartate, and glutamate metabolism, phenylalanine, tyrosine and tryptophan biosynthesis, tyrosine metabolism and carbon fixation in photosynthetic organisms as shown in (Fig. 5D). Phenylalanine, L-tyrosine, and L-tryptophan are amino acids that are ubiquitously involved in protein synthesis. Tryptophan, tyrosine, and phenylalanine all possess phenyl groups and are classified as aromatic compounds because of their heterocyclic indole rings, and the structural and catalytic functions of phenylalanine, L-tyrosine, and L-tryptophan in proteins are well known. For instance, the aromatic rings of these amino acids stabilize polypeptide structures through stacking effects, take part in acid–base catalysis as a component of catalytic triads, and stabilize electron transport during redox reactions in plant cells.[55]

Overall, the majority of the metabolites found in the studied rapeseed belong to flavonoids (30) and terpenoids (17), amino acids, peptides, and analogues (25), and carbohydrates (5) as shown in Fig. 5E. Based on the primary and secondary metabolites, the CaO NPs-responsive metabolites were categorized into two major groups. KEGG pathway enrichment analysis revealed that the top 40 pathways are mainly related to plant defense and antioxidant activity, with the expression of metabolites related to glycolysis, gluconeogenesis, fructose and mannose degradation, alanine metabolism, amino sugar metabolism being determined in the leaves of the rapeseed plant (Fig. 5F). These findings suggest that CaO NP treatment restored the metabolites of the citrate cycle (TCA cycle), biosynthesis of secondary metabolites, metabolic pathway, and carbon metabolism in rapeseed to normal levels of expression that have a key role in the alleviation of drought stress tolerance, and promotes plant growth under drought stress (Fig. 5G). According to the data, CaO NPs showed higher efficiency in promoting plant growth following drought stress. Furthermore, CaO NPs induced common metabolites and showed a marked increase in carbohydrate metabolism and amino acid biosynthesis, indicating the role of CaO NPs in reprogramming the carbon/nitrogen metabolism-related gene expression involved in the alanine, aspartate, and glutamate metabolism. These findings indicate that CaO NPs potentially improve rapeseed growth by reprogramming the amino acid metabolism under drought stress and facilitating the stimulation of growth and the activation of plant defensive mechanisms.[56] Tryptophan, alanine, glutamate, and proline in particular, have been shown to increase the antioxidative metabolism and reduce photosynthetic deficits in plants under biotic and stressful biotic conditions.[57] Thus, we further investigated the involvement of these metabolites in amino acid biosynthesis in rapeseed seedlings with the onset of CaO NP treatment under drought stress.

Specifically, drought resulted in the up-regulation of eight metabolites and down-regulation of 17 metabolites related to amino acids, peptides, and analogues in rapeseed plants (Fig. 6A). Interestingly, CaO NPs exhibited higher expression levels of 23 metabolites and lowered the expression of metabolites related to amino acid biosynthesis, majorly including cysteine/homocysteine, lysine, tryptophan, alanine, glutamate, and proline as compared to the plants subjected to drought stress (Fig. 6B). In addition, the candidate genes involved in the biosynthesis of flavonoids showed high abundance as compared to plants subjected to drought stress (Fig. 6C). CaO NPs under drought-induced up-regulation of upstream genes such as *CHS*, *CHI*, *F3'H*, and *F3H* in rapeseed plants resulted in a 2.71-fold change, 4.56-fold change, 3.11-fold change, and 2.09-fold change in flavonoid biosynthesis expression (Fig. 6C). In addition, CaO NPs increased the expression of early development genes such as *PAL*, *C4H*, *4CL1*, *4CL5*, *DFR*, and *ANS* by 3.02, 4.15, 2.04, 2.26, 1.55, 0.58-fold changes and late development genes *UGT78D2*, *UGT79B1*, *MT*, *PAP1*, *PAP2* showed upregulated expression by 2.32, 4.0, 2.6, 5.5 and 5.62-fold changes, respectively (Fig. 6C). This

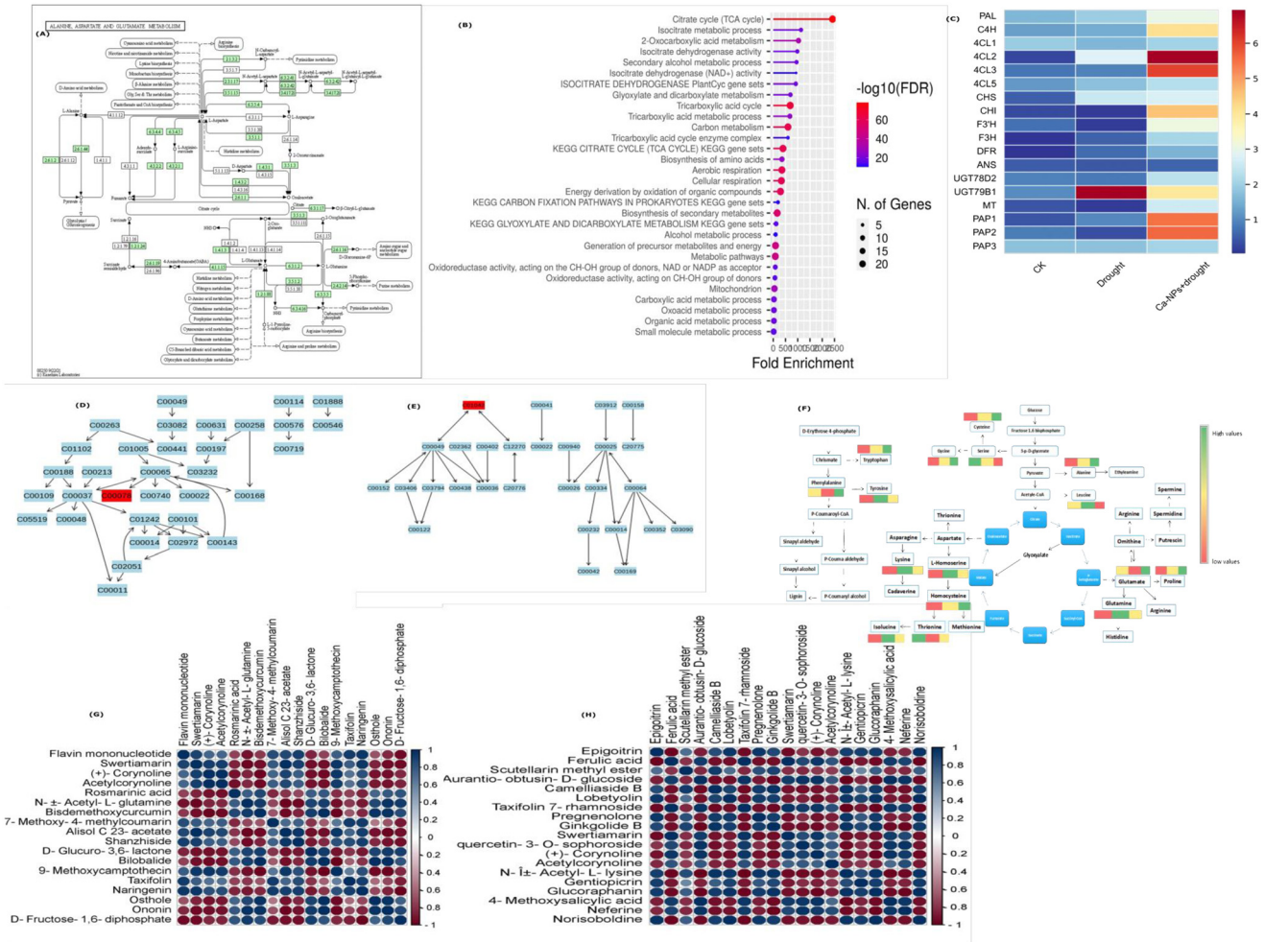

Fig. 6 A schematic representation of the amino acid metabolic pathway (A), metabolic KEGG pathway enrichment of various metabolites ($P > 0.05$) modulated in rapeseed primary and secondary metabolism (B). Analysis of the pathways of phenylpropanoid and flavonoid biosynthesis gene expression after rapeseed onset to the foliar application of 100 mg L^{-1} CaO NPs and 15% PEG-6000 (C). The color bar represents the log 2 expression levels (FPKM, fragments per kilobase of exon per million fragments mapped) of each gene. Expression of hub genes and related metabolite accumulation in the leaf tissue of rapeseed seedlings onset to CaO NPs and drought stress conditions as compared to the control (D–F). The color bar represents log 2 expression levels, while yellow, red, and green boxes represent the metabolite expression (high or low) under control, drought and CaO NPs treatments (left to right), respectively. (G and H) Positive and negative correlation between active molecules under CaO NPs and drought treatments, respectively.

further confirmed the key role of CaO NPs in regulating the growth and stress alleviation in rapeseed by enhancing the activity of major glycosyl-transferases in the flavonol 3-*O*-glycosylation of plants as described in (Fig. 6C). According to our observations, in response to drought conditions, anthocyanin and flavonoid compounds increased in rapeseed following Ca-NPs treatment, counteracting an increase in oxidative stress, which may be a strategy for reducing excessive ROS formation. In this regard, the increase in antioxidant flavonoid compounds in leaves was observed as a part of the induced response to oxidative stress.[58]

Phenylalanine ammonia-lyase (*PAL*) participates in the primary metabolism in the phenylpropanoid pathway, which occurs in the biosynthesis of lignin and flavonoids.[59] At the beginning of the flavonoid pathway, chalcone synthase (*CHS*) produces an intermediate that is utilized in the synthesis of all flavonoids. The isomerization of naringenin chalcone to the flavanone naringenin is catalyzed by the enzyme chalcone isomerase (*CHI*). Flavanone 3-hydroxylase then hydroxylates naringenin to produce dihydrokaempferol. Flavonol synthase (*FLS*) produces flavonol from dihydrokaempferol or dihydroquercetin, while dihydroflavonol 4-reductase produces anthocyanin (*DFR*). The key flavonoid pathway enzymes, such as *CHS*, *CHI*, *F3H*, *F3'H*, *DFR*, *ANS*, and anthocyanin reductase, are all encoded by single genes with the exception of *FLS*, which is responsible for the production of flavonol. Similarly, pretreatment with Spm induced drought tolerance *in vitro* in citrus plants *via* the modification of phenylpropanoid and flavonoid biosynthesis

genes and stomatal activity.[60] Rapeseed metabolomics revealed a diverse set of compounds in response to CaO NPs under drought stress, including secondary metabolites other than flavonoids, carboxylic acids (amino acids and derivatives), prenol lipids (terpenoids), benzene and derivatives, indoles and derivatives, organo-oxygen compounds (carbohydrates), and phenols. It was suggested that Ca-NPs considerably enhanced the accumulation of anthocyanin and flavonoids in rapeseed, where the overall collective actions mitigated the negative impacts of drought stress.

The role of hub genes (Fig. 6D and E), related to plant growth under CaO NPs treatment revealed *B. napus* stress resistance. Fig. 6F shows the expression of active molecules, *e.g.*, amino acids, in carbohydrate metabolism. Likewise, Fig. 6G and H indicate strong positive and negative correlations between active molecules under CaO NPs and drought treatments, which facilitate plant growth and drought tolerance. The application of cerium oxide nanoparticles led to significant changes, mainly in metabolic processes, in wheat seedlings under drought stress. These alterations affected carbohydrate metabolism, inositol phosphate metabolism, ascorbate/aldarate metabolism, methane metabolism, glyoxylate and dicarboxylate metabolism, as well as the tricarboxylic acid (TCA) cycle.[16] Nitrogen metabolism was impacted, resulting in shifts in amino acid pools and nitrogen-containing compounds such as 4-aminobutyric acid, glutamic acid, and putrescine. Interestingly, when combined with our physiological data, substantial alterations were detected in the CaO NP treatment, despite metabolomics data revealing that there were distinct modifications that might be highly significant in a full life cycle study of plants in the field.

3.6 The responsive metabolic signature of CaO NPs in plant secondary metabolism

The responsive secondary metabolites of CaO NPs markedly differed in rapeseed plants following drought stress (Fig. 7A–E). Drought-treated plants showed the down-regulation of 28 metabolites related to carboxylic acids and derivatives, 18 metabolites related to flavonoids, 10 metabolites related to prenol lipids, 7 metabolites related to benzene and derivatives, 4 metabolites related to indoles and derivatives, and 6 metabolites related to phenols (Fig. 7F). CaO NPs treatment up-regulated the expression of common metabolites that were down-regulated in drought (Fig. 8A–D). For example, CaO NPs resulted in the up-regulation of 27 metabolites related to carboxylic acids and derivatives and flavonoids such as taxifolin, ipriflavone, apigenin and naringenin, prenol lipids in the form of terpenoids such as gibberellic acid, bilobalide, and swertiamarin (Fig. 8E). In addition to benzene and derivatives, including 2-phenylbutyric acid, 5-aminosalicylic acid, and 3-methoxyphenylacetic acid, indole and derivatives (serotonin and L-5-hydroxytryptophan), and a distinct phenolic signature were found with CaO NPs treatment, and positive changes were noted for a downstream flavonoid sub-class (anthocyanin), along with non-flavonoid compounds over-represented by lignin. Furthermore, the majority of common metabolites that were downregulated under drought but upregulated in CaO NPs-treated plants belong to the two aforementioned metabolic groups (Fig. 8F), implying their potential role in the metabolomics-based discrimination of CaO NPs-responsive metabolites in rapeseed under drought stress. According to previous studies, methionine is the most common low molecular weight sulfur-containing amino acid and is a crucial antioxidant for the defense mechanisms, gene expression, and signal transduction in plants.[61] A frequent physiological reaction to abiotic stress is proline activation. Along with carbohydrates, proteins, and amino acids, plants also contain several compounds that are regarded to be "defense-promoting" including anthocyanins, flavonoids, and other phenolics.[62] These substances may play a role in scavenging ROS that are produced in plants under various stress conditions and cause oxidative stress. However, at the 100 mg L^{-1} CaO NPs dose, the activation of the aforementioned metabolic pathways might boost plant performance, particularly under diverse stressors. Flavonoids, on the other hand, function as regulators of plant growth, attracting pollinator insects and protecting against biotic and abiotic stresses.[63] Following that, metabolomics studies identified the mechanism through which CaO NPs promoted drought tolerance in rapeseed seedlings. This work suggests that metallic nanoparticles can act as plant growth regulators and sheds new light on how metal nanoparticles might be used to benefit crops in water-stressed areas.

4. Conclusion

This study has examined the role of CaO NPs in plant growth regulation and the drought tolerance response of rapeseed seedlings. CaO NPs considerably influenced the metabolic pathways by reprogramming the key metabolites, including flavonoids, terpenoids, amino acids, phytohormones, phenol, phenylpropanoids, carbohydrates, amines, alcohols, coumarins and derivatives, quinone, polyketides, fatty acids, sterol lipids, prenol lipids, organic acids, benzene and derivatives, indole, and imidazoles, and the involved metabolites were significantly correlated with the plant growth. CaO NPs resulted in the up-regulated expression of upstream genes (*CHS*, *CHI*, *F3′H*, *F3H*) related to flavonoid biosynthesis. Notably, CaO NPs recovered the metabolites to normal levels under drought stress. In addition, the expression enrichment of early development genes, such as *PAL*, *C4H*, *4CL1*, *4CL5*, *DFR*, *ANS*, and late development genes, *UGT78D2*, *UGT79B1*, *MT*, *PAP1*, *PAP2*, in CaO NPs treatment further confirmed its role in plant growth and stress

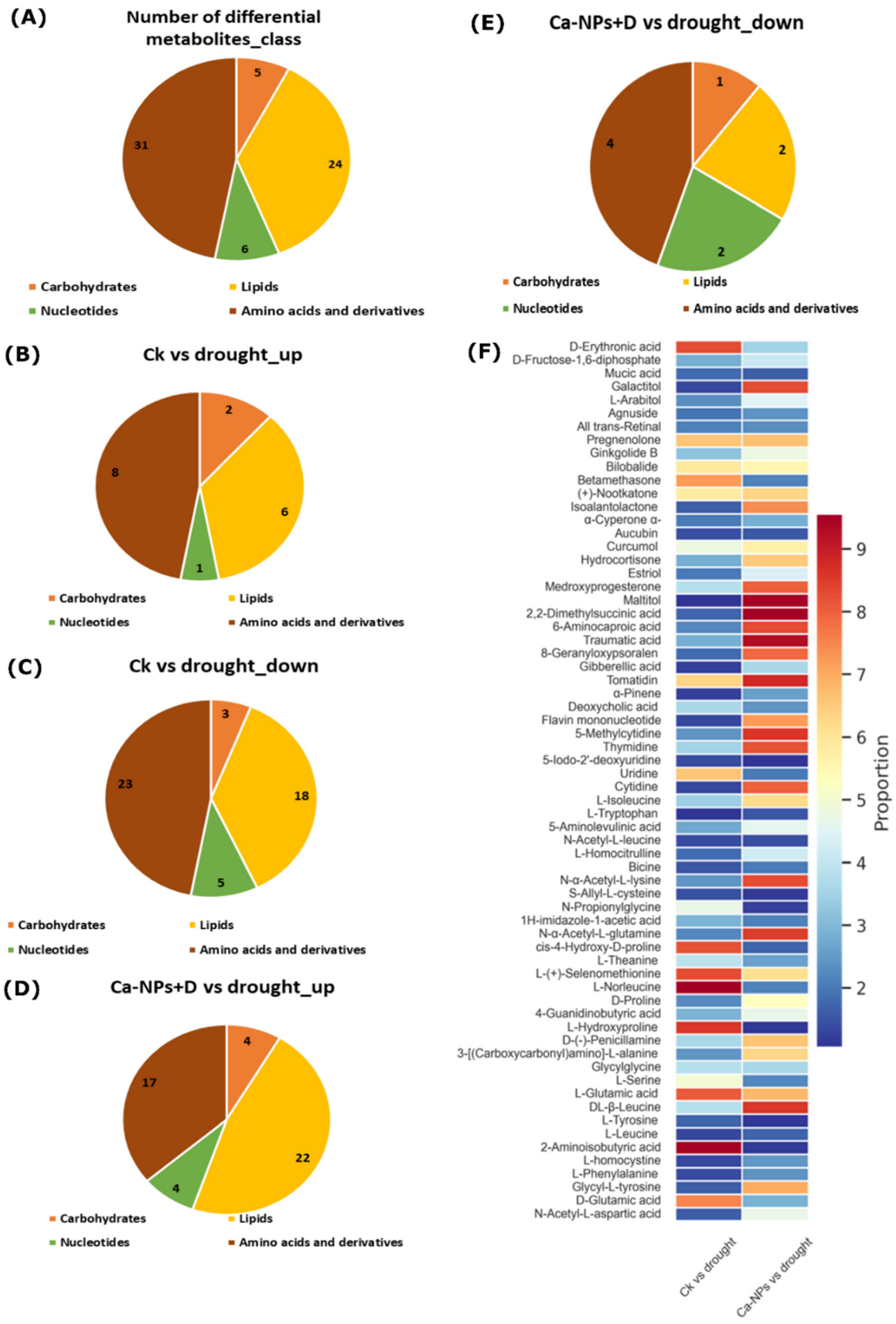

Fig. 7 The general profile of differential metabolites selectively modulated in the primary and secondary metabolism of rapeseed after foliar treatment with 100 mg L^{-1} CaO NPs and 15% PEG-6000 for 7 days (A–E). Differential metabolite expression in *control vs. drought* and *CaO NPs + D vs. drought* treatments specifically regulated in the primary metabolism and secondary metabolism of rapeseed. (F) Differential metabolite expression in *control vs. drought* specifically regulated in the primary metabolism of rapeseed. Each metabolite's log 2 expression levels are shown by the color bar.

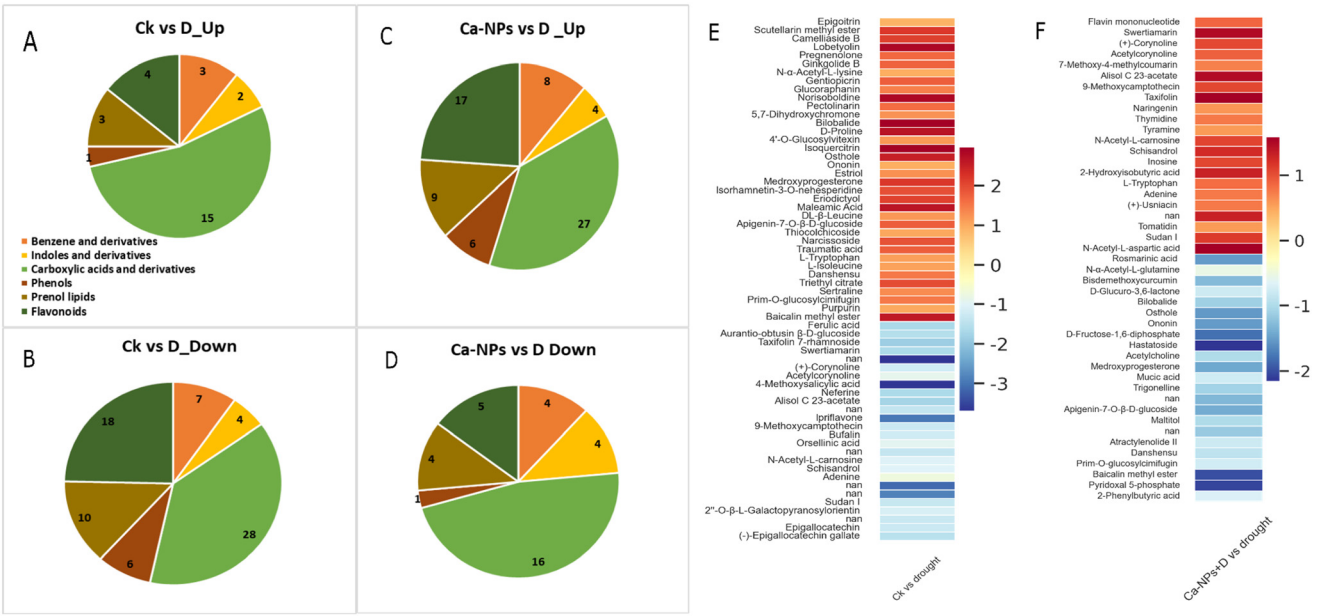

Fig. 8 Taxonomical characterization of differential secondary metabolites in rapeseed seedlings under drought and CaO NP treatment (15% PEG-6000) conditions. (A–D) A representation of the number of up-regulated and down-regulated metabolites for each designated class, *i.e.*, carboxylic acids and derivatives, flavonoids, prenol lipids, benzene and derivatives, indoles and derivatives, and phenols under control *vs.* drought stress conditions. (E and F) The differential metabolite expression in *control vs. drought* and *CaO NPs + D vs. drought* treatments specifically regulated in the secondary metabolism of rapeseed, respectively. The color bar represents the log 2 expression levels of each metabolite.

alleviation by enhancing the major glycosyl-transferases involved in flavonol 3-*O*-glycosylation in the leaves of plants as illustrated in Fig. 6. The findings of this study enable us to elucidate the CaO NPs-mediated mechanism by reprogramming the metabolome profile and provide novel insights into CaO NPs for regulating rapeseed growth under drought stress. Further studies on the involved molecular mechanism of CaO NP-mediated treatment are required in rapeseed, which will allow us to provide compelling evidence for using nanomaterials in plant growth and agricultural yield.

Data availability

All data presented in this study is available in the article and ESI.†

Author contributions

Ahsan Ayyaz and Iram Batool: methodology, validation, formal analysis, investigation, data curation, and writing – original draft; Kangni Zhang, Fakhir Hannan, Tongjun Qin: validation, investigation. data curation; Yongqi Sun, Habib-ur-Rehman Athar, Zafar Ullah Zafar: investigation; Muhammad Ahsan Farooq: methodology, formal analysis, writing – review & editing; Weijun Zhou: conceptualization, resources, writing – review & editing, supervision, project administration, funding acquisition.

Conflicts of interest

The authors declare that they have no known competing financial interests or personal relationships that could have appeared to influence the work reported in this paper.

Acknowledgements

This work was supported by the Science and Technology Department of Zhejiang Province (2023C02002-3), Collaborative Innovation Center for Modern Crop Production co-sponsored by Province and Ministry (CIC-MCP), and Agriculture and Rural Affairs Department of Zhejiang Province (2023ZDXT01). We thank Weizhen Hu and Deli Sun from Agricultural Experiment Station of Zhejiang University for their assistance.

References

1 M. Ashraf and H.-U.-R. Athar, Preface, *Pak. J. Bot.*, 2006, **38**, 1357.
2 C. H. Foyer and I. Kranner, Plant adaptation to climate change, *Biochem. J.*, 2023, **480**, 1865–1869.
3 W. Xiong, M. Reynolds and Y. Xu, Climate change challenges plant breeding, *Curr. Opin. Plant Biol.*, 2022, **70**, 102308.
4 N. Ndlovu, T. Mayaya, C. Muitire and N. Munyengwa, Nanotechnology applications in crop production and food systems, *Int. J. Plant Breed.*, 2020, **7**, 624–634.

5 A. Wahab, A. Munir, M. H. Saleem, M. I. AbdulRaheem, H. Aziz, M. F. B. Mfarrej and G. Abdi, Interactions of Metal-Based Engineered Nanoparticles with Plants: An Overview of the State of Current Knowledge, Research Progress, and Prospects, *J. Plant Growth Regul.*, 2023, **42**, 5396–5416.
6 B. Zhang, Y. Gao, L. Zhang and Y. Zhou, The plant cell wall: Biosynthesis, construction, and functions, *J. Integr. Plant Biol.*, 2021, **63**, 251–272.
7 P. Manishankar, N. Wang, P. Köster, A. A. Alatar and J. Kudla, Calcium signaling during salt stress and in the regulation of ion homeostasis, *J. Exp. Bot.*, 2018, **69**, 4215–4226.
8 X. Weng, H. Li, C. Ren, Y. Zhou, W. Zhu, S. Zhang and L. Liu, Calcium regulates growth and nutrient absorption in poplar seedlings, *Front. Plant Sci.*, 2022, **13**, 887098.
9 S. Aras, H. Keles and E. Bozkurt, Physiological and histological responses of peach plants grafted onto different rootstocks under calcium deficiency conditions, *Sci. Hortic.*, 2021, **281**, 109967.
10 A. Singh, S. Tiwari, J. Pandey, C. Lata and I. K. Singh, Role of nanoparticles in crop improvement and abiotic stress management, *J. Biotechnol.*, 2021, **337**, 57–70.
11 A. C. P. de Moraes and P. T. Lacava, in *Silicon and Nano-silicon in Environmental Stress Management and Crop Quality Improvement*, Elsevier, 2022, pp. 55–65.
12 K. K. Verma, X.-P. Song, Z.-L. Chen, D.-D. Tian, V. D. Rajput, M. Singh, T. Minkina and Y.-R. Li, in *Silicon and Nano-silicon in Environmental Stress Management and Crop Quality Improvement*, Elsevier, 2022, pp. 207–218.
13 M. W. Mazhar, M. Ishtiaq, M. Maqbool and R. Akram, Seed priming with Calcium oxide nanoparticles improves germination, biomass, antioxidant defence and yield traits of canola plants under drought stress, *S. Afr. J. Bot.*, 2022, **151**, 889–899.
14 M. M. Nazir, M. Noman, T. Ahmed, S. Ali, Z. Ulhassan, F. Zeng and G. Zhang, Exogenous calcium oxide nanoparticles alleviate cadmium toxicity by reducing Cd uptake and enhancing antioxidative capacity in barley seedlings, *J. Hazard. Mater.*, 2022, **438**, 129498.
15 A. Ayyaz, R. Fang, J. Ma, F. Hannan, Q. Huang, H.-U.-R. Athar, Y. Sun, M. Javed, S. Ali, W. Zhou and M. A. Farooq, Calcium nanoparticles (Ca-NPs) improve drought stress tolerance in Brassica napus by modulating the photosystem II, nutrient acquisition and antioxidant performance, *NanoImpact*, 2022, **28**, 100423.
16 C. M. Rico, D. Wagner, O. Abolade, B. Lottes and K. Coates, Metabolomics of wheat grains generationally-exposed to cerium oxide nanoparticles, *Sci. Total Environ.*, 2020, **712**, 136487.
17 X. Guo, Z. Xin, T. Yang, X. Ma, Y. Zhang, Z. Wang, Y. Ren and T. Lin, Metabolomics response for drought stress tolerance in chinese wheat genotypes (Triticum aestivum), *Plants*, 2020, **9**, 520.
18 M. A. Farooq, K. Zhang, F. Islam, J. Wang, H. U. Athar, A. Nawaz, Z. Ullah Zafar, J. Xu and W. Zhou, Physiological and itraq-based quantitative proteomics analysis of methyl jasmonate–induced tolerance in Brassica napus under arsenic stress, *Proteomics*, 2018, **18**, 1700290.
19 Q. Zheng and K. Liu, Worldwide rapeseed (Brassica napus L.) research: A bibliometric analysis during 2011–2021, *Oil Crop Science*, 2022, **7**, 157–165.
20 J. Zhu, D. Cai, J. Wang, J. Cao, Y. Wen, J. He, L. Zhao, D. Wang and S. Zhang, Physiological and anatomical changes in two rapeseed (Brassica napus L.) genotypes under drought stress conditions, *Oil Crop Science*, 2021, **6**, 97–104.
21 A. Minta, J. P. Kao and R. Y. Tsien, Fluorescent indicators for cytosolic calcium based on rhodamine and fluorescein chromophores, *J. Biol. Chem.*, 1989, **264**, 8171–8178.
22 B. Yazıcılar, F. Böke, A. Alaylı, H. Nadaroglu, S. Gedikli and I. Bezirganoglu, In vitro effects of CaO nanoparticles on Triticale callus exposed to short and long-term salt stress, *Plant Cell Rep.*, 2021, **40**, 29–42.
23 D. I. Arnon and F. Whatley, Is chloride a coenzyme of photosynthesis?, *Science*, 1949, **110**, 554–556.
24 A. Ayyaz, Y. Miao, F. Hannan, F. Islam, K. Zhang, J. Xu, M. A. Farooq and W. Zhou, Drought tolerance in Brassica napus is accompanied with enhanced antioxidative protection, photosynthetic and hormonal regulation at seedling stage, *Physiol. Plant.*, 2021, **172**, 1133–1148.
25 A. Ayyaz, Y. Zhou, I. Batool, F. Hannan, Q. Huang, K. Zhang, K. Shahzad, Y. Sun, M. A. Farooq and W. Zhou, Calcium nanoparticles and abscisic acid improve drought tolerance, mineral nutrients uptake and inhibitor-mediated photosystem II performance in Brassica napus, *J. Plant Growth Regul.*, 2024, **43**, 516–537.
26 K.-J. Appenroth, J. Stöckel, A. Srivastava and R. Strasser, Multiple effects of chromate on the photosynthetic apparatus of Spirodela polyrhiza as probed by OJIP chlorophyll a fluorescence measurements, *Environ. Pollut.*, 2001, **115**, 49–64.
27 H. Bano, H. U. R. Athar, Z. U. Zafar, H. M. Kalaji and M. Ashraf, Linking changes in chlorophyll a fluorescence with drought stress susceptibility in mung bean [Vigna radiata (L.) Wilczek], *Physiol. Plant.*, 2021, **172**, 1244–1254.
28 J. Ma, F. Islam, A. Ayyaz, R. Fang, F. Hannan, M. A. Farooq, B. Ali, Q. Huang, R. Sun and W. Zhou, Wood vinegar induces salinity tolerance by alleviating oxidative damages and protecting photosystem II in rapeseed cultivars, *Ind. Crops Prod.*, 2022, **189**, 115763.
29 K. Vijai Anand, M. Reshma, M. Kannan, S. Muthamil Selvan, S. Chaturvedi, A. E. Shalan and K. Govindaraju, Preparation and characterization of calcium oxide nanoparticles from marine molluscan shell waste as nutrient source for plant growth, *J. Nanostruct. Chem.*, 2021, 1–14.
30 A. Dutta, Fourier transform infrared spectroscopy, *Spectroscopic methods for nanomaterials characterization*, 2017, pp. 73–93.
31 N. Vijayakumar, S. K. Venkatraman, S. Imthiaz, E. A. Drweesh, M. M. Elnagar, S. Koppala and S. Swamiappan, Synthesis and characterization of calcium and magnesium based oxides and titanates for photocatalytic degradation of rhodamine B: A comparative study, *Sci. Rep.*, 2023, **13**, 3615.

32 M. Simsek, B. Yazicilar, F. Boke, H. Nadaroglu and A. Alayli, *Assessment of the Effects of Newly Fabricated CaO, CuO, ZnO Nanoparticles on Callus Formation Maintainance of Alfalfa (Medicago Sativa L.) Under In Vitro Salt Stress*, 2021.
33 H. Nadaroglu, H. C. Kaymak, A. Alayli and K. A. T. Kapakin, Investigation of Potential Antioxidative Effects of CaO Nanoparticles On Bean Seeds (Phaseolus vulgaris L.), *Gesunde Pflanz.*, 2023, **75**, 289–301.
34 P. Hu, J. An, M. M. Faulkner, H. Wu, Z. Li, X. Tian and J. P. Giraldo, Nanoparticle Charge and Size Control Foliar Delivery Efficiency to Plant Cells and Organelles, *ACS Nano*, 2020, **14**, 7970–7986.
35 Q. Huang, A. Ayyaz, M. A. Farooq, K. Zhang, W. Chen, F. Hannan, Y. Sun, K. Shahzad, B. Ali and W. Zhou, Silicon dioxide nanoparticles enhance plant growth, photosynthetic performance, and antioxidants defence machinery through suppressing chromium uptake in Brassica napus L, *Environ. Pollut.*, 2024, **342**, 123013.
36 C. O. Dimkpa, U. Singh, P. S. Bindraban, W. H. Elmer, J. L. Gardea-Torresdey and J. C. White, Zinc oxide nanoparticles alleviate drought-induced alterations in sorghum performance, nutrient acquisition, and grain fortification, *Sci. Total Environ.*, 2019, **688**, 926–934.
37 M. I. Ghani, S. Saleem, S. A. Rather, M. S. Rehmani, S. Alamri, V. D. Rajput, H. M. Kalaji, N. Saleem, T. A. Sial and M. Liu, Foliar application of zinc oxide nanoparticles: An effective strategy to mitigate drought stress in cucumber seedling by modulating antioxidant defense system and osmolytes accumulation, *Chemosphere*, 2022, **289**, 133202.
38 A. K. Nasrallah, A. A. Kheder, M. A. Kord, A. S. Fouad, M. M. El-Mogy and M. A. Atia, Mitigation of salinity stress effects on broad bean productivity using calcium phosphate nanoparticles application, *Horticulturae*, 2022, **8**, 75.
39 H. Manzoor, Mehwish, S. Bukhat, S. Rasul, M. I. A. Rehmani, S. Noreen, H.-U.-R. Athar, Z. U. Zafar, M. Skalicky, W. Soufan, M. Brestic, M. Habib-ur-Rahman, C. C. Ogbaga and A. EL Sabagh, Methyl Jasmonate Alleviated the Adverse Effects of Cadmium Stress in Pea (Pisum sativum L.): A Nexus of Photosystem II Activity and Dynamics of Redox Balance, *Front. Plant Sci.*, 2022, **13**, 860664.
40 M. Javed, M. Iqbal, H.-U.-R. Athar, Z. U. Zafar, F. Arshad and M. Ashraf, Role of photosystem II activity in salt tolerance of Panicum antidotale and Panicum turgidum: Insights from chlorophyll a fluorescence analysis on excised leaf, *J. Anim. Plant Sci.*, 2024, **34**, 387–399.
41 M. Javed, M. Iqbal, H. Bano, N. Hussain, A. Ghaffar, Z. U. Zafar, A. Hussain, M. Abdullah, A. Ayyaz, M. A. Farooq, M. Ashraf and H. R. Athar, Photosynthetic acclamatory response of Panicum antidotale Retz. populations to root zone desiccation stress, *Braz. J. Microbiol.*, 2024, **84**, e252735.
42 F. S. Mirza, Z.-E.-H. Aftab, M. D. Ali, A. Aftab, T. Anjum, H. Rafiq and G. Li, Green synthesis and application of GO nanoparticles to augment growth parameters and yield in mungbean (Vigna radiata L.), *Front. Plant Sci.*, 2022, **13**, 1040037.
43 Y. Gao, S. Chen, Y. Li and Y. Shi, Effect of nano-calcium carbonate on morphology, antioxidant enzyme activity and photosynthetic parameters of wheat (Triticum aestivum L.) seedlings, *Chem. Biol. Technol. Agric.*, 2023, **10**, 31.
44 H. Bano, H. U. R. Athar, Z. U. Zafar, C. C. Ogbaga and M. Ashraf, Peroxidase activity and operation of photo-protective component of NPQ play key roles in drought tolerance of mung bean [Vigna radiata (L.) Wilczek], *Physiol. Plant.*, 2021, **172**, 603–614.
45 M. Grieco, V. Roustan, G. Dermendjiev, S. Rantala, A. Jain, M. Leonardelli, K. Neumann, V. Berger, D. Engelmeier and G. Bachmann, Adjustment of photosynthetic activity to drought and fluctuating light in wheat, *Plant, Cell Environ.*, 2020, **43**, 1484–1500.
46 S. H. Raza, H. U. R. Athar and M. Ashraf, Influence of exogenously applied glycinebetaine on the photosynthetic capacity of two differently adapted wheat cultivars under salt stress, *Pak. J. Bot.*, 2006, **38**, 341–351.
47 A. Kausar, S. Hussain, T. Javed, S. Zafar, S. Anwar, S. Hussain, N. Zahra and M. Saqib, Zinc oxide nanoparticles as potential hallmarks for enhancing drought stress tolerance in wheat seedlings, *Plant Physiol. Biochem.*, 2023, **195**, 341–350.
48 Y. Wang, S. Chen, C. Deng, X. Shi, K. Cota-Ruiz, J. C. White, L. Zhao and J. L. Gardea-Torresdey, Metabolomic analysis reveals dose-dependent alteration of maize (Zea mays L.) metabolites and mineral nutrient profiles upon exposure to zerovalent iron nanoparticles, *NanoImpact*, 2021, **23**, 100336.
49 Z. Nie, L. Wang, P. Zhao, Z. Wang, Q. Shi and H. Liu, Metabolomics reveals the impact of nitrogen combined with the zinc supply on zinc availability in calcareous soil via root exudates of winter wheat (Triticum aestivum), *Plant Physiol. Biochem.*, 2023, **204**, 108069.
50 D. C. Johnson, D. R. Dean, A. D. Smith and M. K. Johnson, Structure, function, and formation of biological iron-sulfur clusters, *Annu. Rev. Biochem.*, 2005, **74**, 247–281.
51 S. Khadem and R. J. Marles, Monocyclic phenolic acids; hydroxy-and polyhydroxybenzoic acids: occurrence and recent bioactivity studies, *Molecules*, 2010, **15**, 7985–8005.
52 B. Chanda, Y. Xia, M. K. Mandal, K. Yu, K. T. Sekine, Q.-M. Gao, D. Selote, Y. Hu, A. Stromberg and D. Navarre, Glycerol-3-phosphate is a critical mobile inducer of systemic immunity in plants, *Nat. Genet.*, 2011, **43**, 421–427.
53 H. Lim, M.-H. Cho, S. H. Bhoo and T.-R. Hahn, Pyrophosphate: fructose-6-phosphate 1-phosphotransferase is involved in the tolerance of Arabidopsis seedlings to salt and osmotic stresses, *In Vitro Cell. Dev. Biol.: Plant*, 2014, **50**, 84–91.
54 M. W. Mazhar, M. Ishtiaq, M. Maqbool, S. Atiq Hussain, R. Casini, A. M. Abd-ElGawad and H. O. Elansary, Seed Nano-Priming with Calcium Oxide Maintains the Redox State by Boosting the Antioxidant Defense System in Water-Stressed Carom (Trachyspermum ammi L.) Plants to Confer Drought Tolerance, *Nanomaterials*, 2023, **13**, 1453.
55 J. Barros and R. A. Dixon, Plant phenylalanine/tyrosine ammonia-lyases, *Trends Plant Sci.*, 2020, **25**, 66–79.
56 S. H. Nile, M. Thiruvengadam, Y. Wang, R. Samynathan, M. A. Shariati, M. Rebezov, A. Nile, M. Sun, B. Venkidasamy and J. Xiao, Nano-priming as emerging seed priming

technology for sustainable agriculture—recent developments and future perspectives, *J. Nanobiotechnol.*, 2022, **20**, 254.
57 T. Bashir, S. A. U. Haq and A. M. Husaini, in *Multiple Abiotic Stress Tolerances in Higher Plants*, CRC Press, 2023, pp. 255–265.
58 M. Al Hassan, J. Chaura, M. Donat-Torres, M. Boscaiu and O. Vicente, *Antioxidant responses under salinity and drought in*, 2017.
59 S. Purwar, S. Sundaram, S. Sinha, A. Gupta, N. Dobriyall and A. Kumar, Expression and in silico characterization of Phenylalanine ammonium lyase against karnal bunt (Tilletia indica) in wheat (Triticum aestivum), *Bioinformation*, 2013, **9**, 1013.
60 R. Jan, S. Asaf, M. Numan, Lubna and K.-M. Kim, Plant secondary metabolite biosynthesis and transcriptional regulation in response to biotic and abiotic stress conditions, *Agronomy*, 2021, **11**, 968.
61 E. Mukwevho, Z. Ferreira and A. Ayeleso, Potential role of sulfur-containing antioxidant systems in highly oxidative environments, *Molecules*, 2014, **19**, 19376–19389.
62 S. Kaur, V. Tiwari, A. Kumari, E. Chaudhary, A. Sharma, U. Ali and M. Garg, Protective and defensive role of anthocyanins under plant abiotic and biotic stresses: An emerging application in sustainable agriculture, *J. Biotechnol.*, 2023, **361**, 12–29.
63 C. Brunetti, M. Di Ferdinando, A. Fini, S. Pollastri and M. Tattini, Flavonoids as antioxidants and developmental regulators: Relative significance in plants and humans, *Int. J. Mol. Sci.*, 2013, **14**, 3540–3555.rho.